Effects of Copper Substitution to Mn-site on Magnetic and Magnetocaloric Properties of La$_{0.7}$Sr$_{0.3}$Mn$_{1-x}$Cu$_x$O$_3$ Manganites

Selda KILIÇ ÇETİN[1], Gönül AKÇA[1,*], Mehmet Selim ASLAN[1], Ahmet EKİCİBİL[1]

[1]*Çukurova University, Faculty of Science and Letters, Department of Physics, 01330, Adana, Türkiye*
kilics@cu.edu.tr, ORCID: 0000-0003-4112-4475
[1]*Çukurova University, Faculty of Science and Letters, Department of Physics, 01330, Adana, Türkiye*
gdayan@cu.edu.tr, ORCID: 0000-0001-7187-9516
[1]*Çukurova University, Faculty of Science and Letters, Department of Physics, 01330, Adana, Türkiye*
mehmetselimaslan34@gmail.com, ORCID NO: 0000-0001-7086-9105
[1]*Çukurova University, Faculty of Science and Letters, Department of Physics, 01330, Adana, Türkiye*
ahmetcan@cu.edu.tr, ORCID NO: 0000-0003-3071-0444

Abstract

In present study, the effects of copper substitution on the magnetic and magnetocaloric properties of La$_{0.7}$Sr$_{0.3}$Mn$_{1-x}$Cu$_x$O$_3$ manganite samples were investigated. La$_{0.7}$Sr$_{0.3}$Mn$_{1-x}$Cu$_x$O$_3$ samples were obtained by using sol-gel method. X-ray diffraction analyses were performed to determine structural properties such as lattice parameters and crystal structure. The crystal structure of the samples is rhombohedral with space group $R\overline{3}c$. The Cu substitution to the Mn-site causes a decrease in the magnetic phase transition temperature (T_C) of the samples. By using Banerjee criterion and Landau theory, the type of magnetic phase transition is determined as second order. From isothermal magnetization measurements, magnetic entropy change (-ΔS_M) values were calculated for different magnetic field changes of the samples. The maximum magnetic entropy change value (-ΔS_M^{max}) determined from the temperature dependence of -ΔS_M curves for the samples is 3.39 and 2.78 JKg^{-1}K^{-1} under 5 T, respectively. Relative cooling power (RCP) values of the samples were found as 249.52 and 111.98 Jkg^{-1} for 5 T, respectively.

Keywords: Magnetic refrigeration; Magnetic entropy change; Curie temperature; Manganite; Landau theory.

Mn Bölgesine Bakır Katkılamasının La$_{0.7}$Sr$_{0.3}$Mn$_{1-x}$Cu$_x$O$_3$ Manganitlerinin Manyetik ve Manyetokalorik Özellikleri Üzerindeki Etkileri

Öz

Bu çalışmada, Cu katkılamasının La$_{0.7}$Sr$_{0.3}$Mn$_{1-x}$Cu$_x$O$_3$ manganit numunelerinin manyetik ve manyetokalorik özelliklerine etkileri incelenmiştir. La$_{0.7}$Sr$_{0.3}$Mn$_{1-x}$Cu$_x$O$_3$ numuneleri sol-jel tekniği kullanılarak elde edilmiştir. Örgü parametreleri ve kristal yapı gibi yapısal parametreleri belirlemek için x-ışını kırınım analizleri yapılmıştır. Numunelerin kristal yapısı, $R\overline{3}c$ uzay grubu ile rombohedraldir. Mn bölgesindeki Cu katkılamasının manyetik faz geçiş sıcaklığını (T_C) düşürdüğü gözlenmiştir. Banerjee kriteri ve Landau teorisi kullanılarak manyetik faz geçişinin türü ikinci dereceden olarak belirlenmiştir. İzotermal manyetizasyon ölçümlerinden numunelerin farklı manyetik alan değişimleri için manyetik entropi değişimi (-ΔS_M) değerleri hesaplanmıştır. Sıcaklığa bağlı -ΔS_M eğrilerinden belirlenen maksimum manyetik entropi değişim (-ΔS_M^{max}) değeri 5 T altında örnekler için sırasıyla 3.39 ve 2.78 Jkg^{-1}K^{-1}' dir. Örneklerin bağıl soğutma gücü (RCP) değerleri 5 T için sırasıyla 249.52 ve 111.98 Jkg^{-1} olarak bulunmuştur.

Anahtar Kelimeler: Manyetik soğutma; Manyetik entropi değişimi; Curie sıcaklığı; Manganit; Landau teorisi.

1. Introduction

Developed and developing societies need various technologies in every field in order to raise their living standards and reach the level of comfort. One of the technologies widely used in almost every time of human life, including before and after, is cooling technologies [1]. Conventional cooling systems used today are technologies based on the principle of compression of gases with known negative effects on environment [2]. Many efforts have been carried out to reduce the negative effects of the gases used as refrigerants in these systems on the environment and to make improvements [3]. In addition to environmental factors, it is imperative to take the necessary steps to increase the energy efficiency of these systems, where energy consumption is high [4]. Efforts to reduce environmental impacts and energy consumption are not easy and inexpensive. Therefore, there is a need to develop and design new systems that can replace these systems [5]. Recently, intensive studies have been performed on magnetic refrigeration (MR) systems, which are accepted as an alternative technology to conventional systems [1, 2, 6]. Various MR systems have been developed; however, commercial use of these systems has not

yet been fully achieved. The most important reason for this is the problems encountered in the supply of materials to be used as cooling elements in these systems. The main purpose of studies performed for MR technologies is to find the best candidate material that can be used as a cooling element in applications of these systems operating according to the magnetocaloric effect (MCE) principle [7-10]. MCE can basically be explained as when a magnetic field is subjected to a magnetic material, the change in the entropy and temperature of the material [11]. For a magnetocaloric material to be considered as a candidate cooling material for applications, the material must meet certain criteria [12]. First, the magnetic entropy and adiabatic temperature change values, which define the magnetocaloric properties of the material, should be high enough to provide high performance under a low magnetic field and operating temperature range. Second, magnetic hysteresis related to the working efficiency of the material should be close to zero [13]. Thermal and magnetic hysteresis are associated with the magnetic phase transition type [13, 14]. The samples showing a first-order magnetic phase transition (FOMT) have large hysteresis, and the transition occurs in a narrow temperature range [15]. For the second-order magnetic phase transition (SOMT), the hysteresis is negligibly small and the transition is usually spread over a broad temperature range [16, 17]. This indicates that the RCP, defined as the amount of energy per unit mass of the magnetocaloric material, can be high [18]. In the operating temperature range, magnetocaloric materials with high RCP have a higher potential to be used as coolants in applications. In addition to the mentioned physical properties, the materials should meet certain economic and environmental merit such as low cost of raw material and synthesizing and not including poisonous or carcinogenic elements [13]. Although many material groups with high magnetic entropy and adiabatic temperature values have been discovered around room temperature, many of them exhibit properties that hinder their commercial use [13, 17, 19]. Manganites formulated with $R_{1-x}M_xMnO_3$ have critical advantages such as high chemical stability, low cost of preparation and raw materials and SOMT [13]. There are many studies describing the properties of manganites in detail and based on these studies [13, 20], it can be said that $La_{1-x}Sr_xMnO_3$ is one of the commonly studied compound systems in term of magnetic and magnetocaloric properties among manganite compounds [20, 21] for various applications such as MR and magnetic hyperthermia [22]. It is known that the magnetic and magnetocaloric properties of manganites are explained by double exchange interaction between Mn ions [20]. There are several factors that affect the physical properties of manganites; the Mn^{3+}/Mn^{4+} ratio, the average ionic radius of the A and/or B -site, oxygen deficiency, doping rate and the method chosen in material preparation are among the most important factors [23, 24]. Based on the information attained from the literature, in our present work, Cu substitution was made in Mn-site in order to bring the transition temperature to room temperature in the $LaSrMnO_3$ system. Sol-gel method

was chosen as the material preparation method because of its various advantages [25]. The effects of Cu substitution on the magnetic and magnetocaloric properties were investigated. To compare the results obtained by Maxwell relation, we calculated the $-\Delta S_M$ of the samples by using Landau theory. The type of magnetic phase transition was determined by Banerjee criteria and Landau parameters.

2. Materials and Methods

To obtained targeted $La_{0.7}Sr_{0.3}Mn_{1-x}Cu_xO_3$ (x = 0.05 and 0.1) manganite compounds, $La(NO_3)_3.6H_2O$, SrO, CuO and $Mn(NO_3)_2.4H_2O$ starting materials were used. Sol-gel method was chosen as material production method. The starting compounds were weighed according to stoichiometric ratios and brought into solution form using suitable solvents. The mixture obtained by mixing the solutions was heated in a magnetic stirrer and stirred continuously. Ethylene glycol and citric acid were added to the mixture to obtain a gel form. The processes of the sol-gel material fabrication technique used to prepare the $La_{0.7}Sr_{0.3}Mn_{1-x}Cu_xO_3$ (x = 0.05 and 0.1) compounds are given in Fig. 1. We have used a similar material fabrication process in our previous study [26]. The obtained samples were named as LSMC-0.05 and LSMC-0.10, respectively, depending on the Cu concentration. To determine the structural, magnetic and magnetocaloric properties of the samples, X-Ray Diffraction (XRD), scanning electron microscopy (SEM), and physical property measurement system (PPMS) were used. XRD measurements of the samples were performed by a Philips PANalytical Empyrean x-ray diffraction meter at room temperature in 0.0131 degree increments over the range of 20 and 80. The crystal structures, lattice parameters and unit cell volume of the samples were analyzed with the Fullprof Programme. The grain size and elemental analysis of the samples were studied with a Scanning Electron Microscope (SEM) including Energy Dispersive X-Ray Spectrometry (EDS). In order to determine the transition temperature of the samples, temperature-dependent magnetization measurements were performed under 10 mT in zero field cooled (ZFC) and field cooled (FC) modes in the temperature range of 5-380 K. The isothermal magnetization measurements dependent magnetic field were carried out around the transition temperatures of the samples up to the field value of 5 T. By using the data obtained from isothermal magnetization measurements, the $-\Delta S_M$ values of the samples and the type of magnetic phase transition were determined. In addition, $-\Delta S_M$ value and magnetic phase transition type were determined according to Landau theory. Obtained experimental and theoretical results were compared with each other.
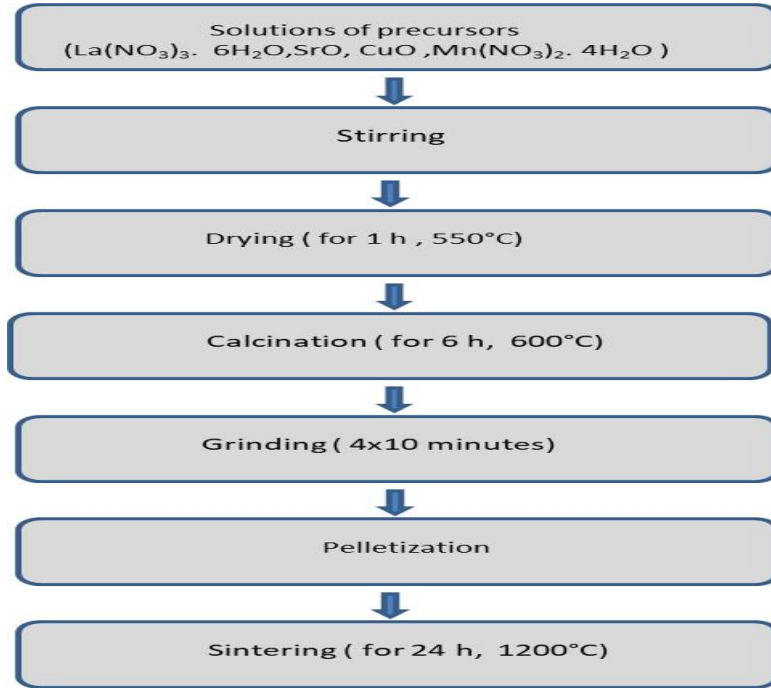
Figure 1: Processes of sol-gel material production technique used to prepare $La_{0.7}Sr_{0.3}Mn_{1-x}Cu_xO_3$ (x = 0.05 and 0.1) compounds

3. Results and Discussion

Figure 2 shows the XRD diffraction patterns of the compounds. It is seen from the XRD diffraction patterns of the samples the narrow-based and sharp diffraction peaks belonging to perovskite structure. The diffraction patterns of the samples have been analyzed in FullProof programs. In the figures, red circle and black line represent the observed and calculated data, respectively. The blue line is difference between them. Green vertical bars show Bragg position. The crystal structure and lattice parameters obtained from the end of analysis for the samples are indicated in Table 1. It is observed that a small change was observed in the lattice parameters and unit cell volume values with the increase of Cu concentration. However, no change has been observed in crystal structure. The perovskite structure is stable at certain values of the tolerance factor given by [27, 28]

$$t = \frac{r_A + r_O}{\sqrt{2}(r_{Mn} + r_O)} \tag{1}$$

equation where r_A *and* $r_{Mn,}$ *a*re the effective radii of the A and Mn site, respectively. r_O represents the effective radii of the O ions. When t values are between 0.96 and 1, it can be said that the crystal structure is rhombohedral [27]. The *t* values of the samples were computed by taking into account Shannon's list of effective ion radii [29]. This value changes from 0.9798 to 0.9806 for
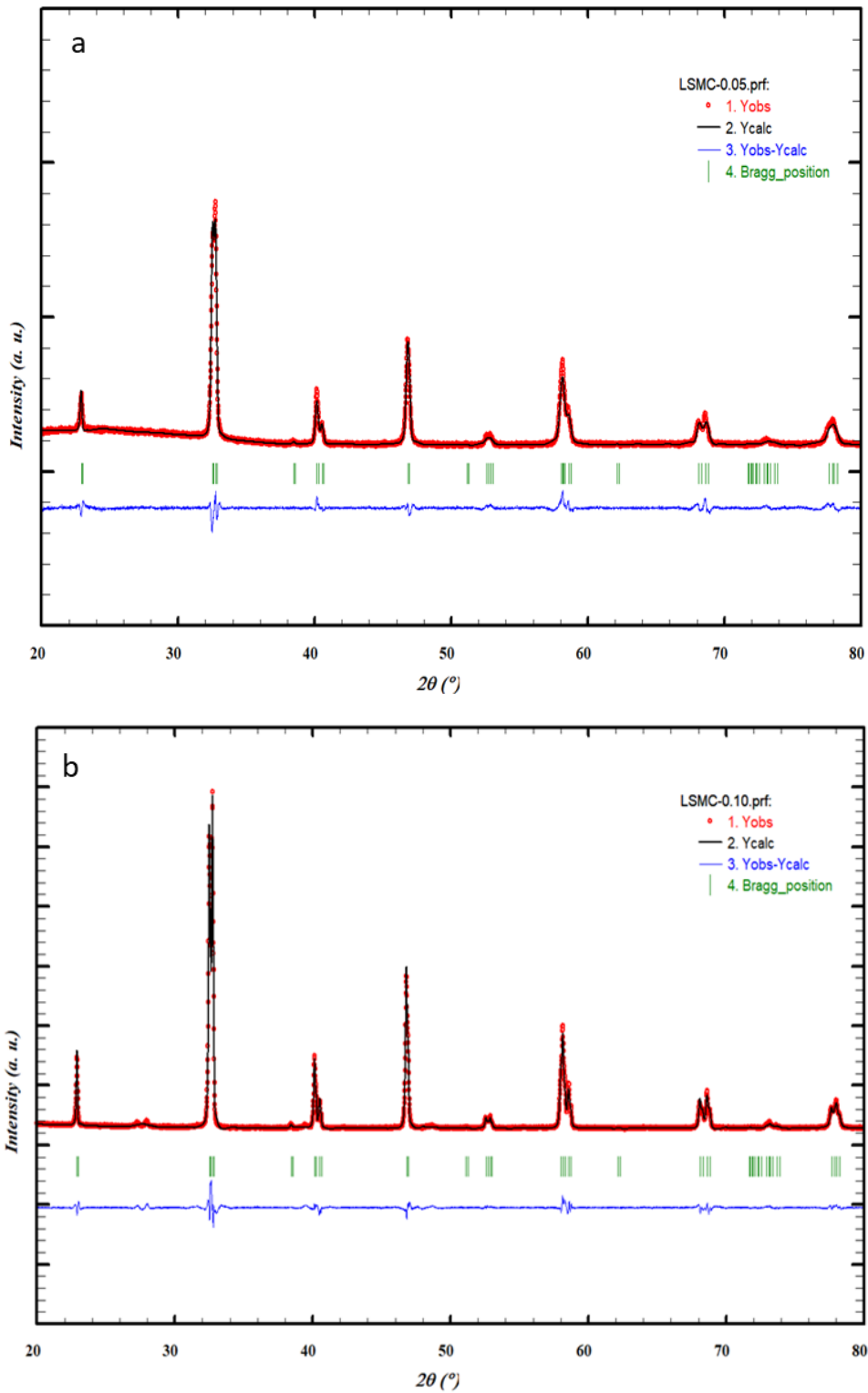
Figure 2: XRD patterns of the samples (a) LSMC-0.05 and (b) LSMC-0.10

LSMC-0.05 and LSMC-0.10, respectively. These values confirm that they crystallize in rhombohedral crystal structures.

Table 1: Lattice parameter obtained from FULLPROF program and grain size of LSMC-0.05 and LSMC-0.10 samples

Sample Code	$a=b$ (Å)	c(Å)	V(Å^3)	d_{Mn-O} (Å)	$\theta_{Mn-O-Mn}$ (°)	*Grain Size (μm)*
LSMC-0.05	5.5073	13.3659	351.0815	1.9498	175.662	0.65
LSMC-0.10	5.5015	13.3449	349.7915	1.9505	175.654	0.47

In Figure 3, SEM images of the LSMC-0.05 and LSMC-0.10 samples are given. For Cu doped samples, different polygonal grain structures of different sizes, definite grain boundaries and mostly oval-like are seen. It is observed that the shape and size of the grains are not homogeneous and there is porosity between the grains. For the LSMC-0.05 sample, the size of the particles varies from 0.20 to 1.94 μm and the average particle size was calculated as 0.645 μm. From SEM images of LSMC-0.10 sample, it is seen that the clarity of the grain boundaries deteriorates. The size of the grains varied between 0.153 and 2.02 μm and the average particle size was calculated as 0.469 μm. It is observed that the grain size of the samples decreased with the increase of Cu concentration. The observed decrement in grain size may cause a variation in magnetic and magnetocaloric properties.
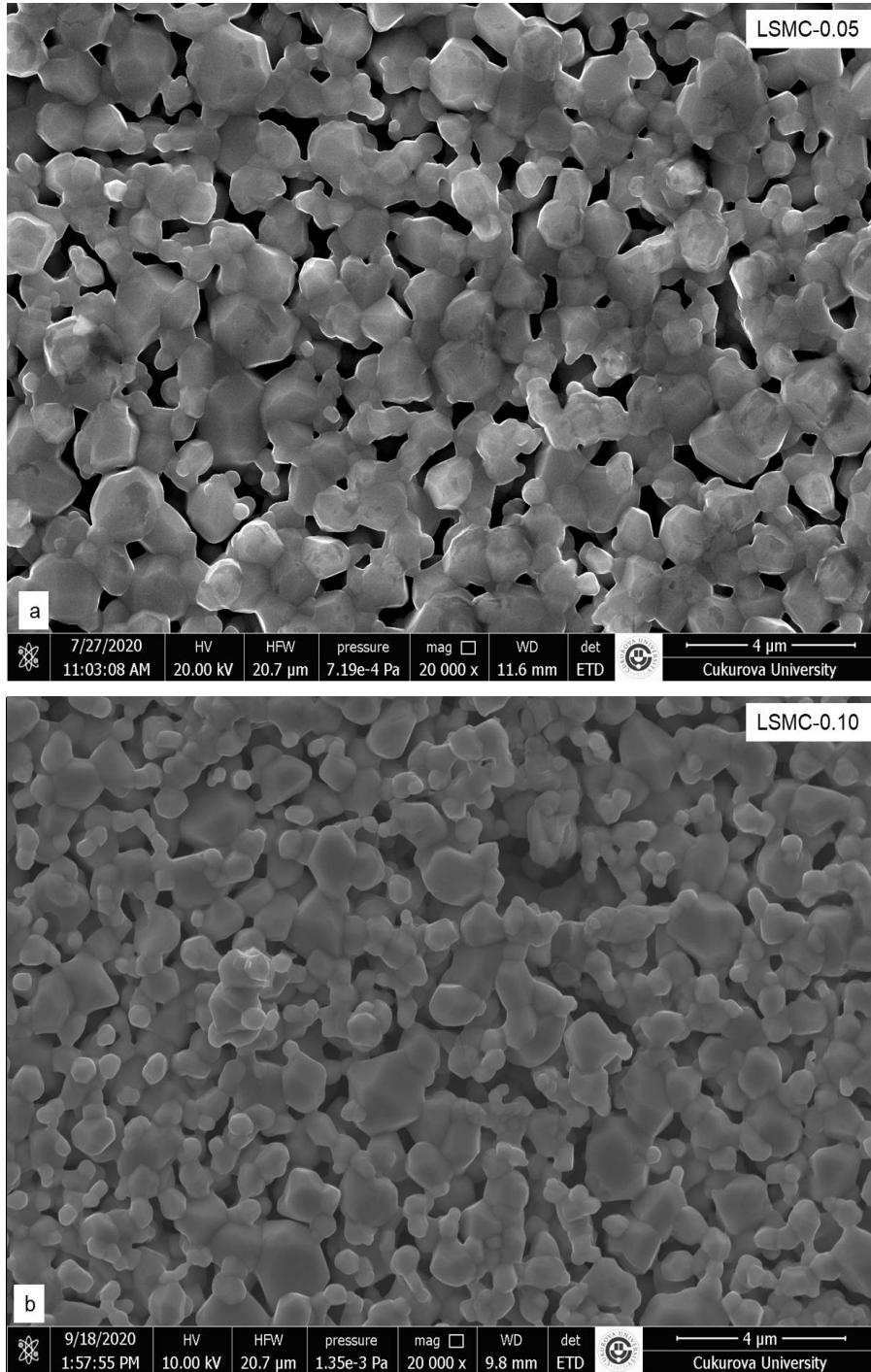
Figure 3: SEM images obtained at 20 kX magnifications of the samples (a) LSMC-0.05 and (b) LSMC-0.10

Figure 4 shows the EDS spectra of the samples. It is observed that the samples contain all expected elements and there are no traces of foreign elements that may interfere with the compound during the preparation and heat treatment process. The atomic percentages of the elements that compose the samples are summarized in Table 2. The obtained results are close to the expected atomic ratios for all samples.
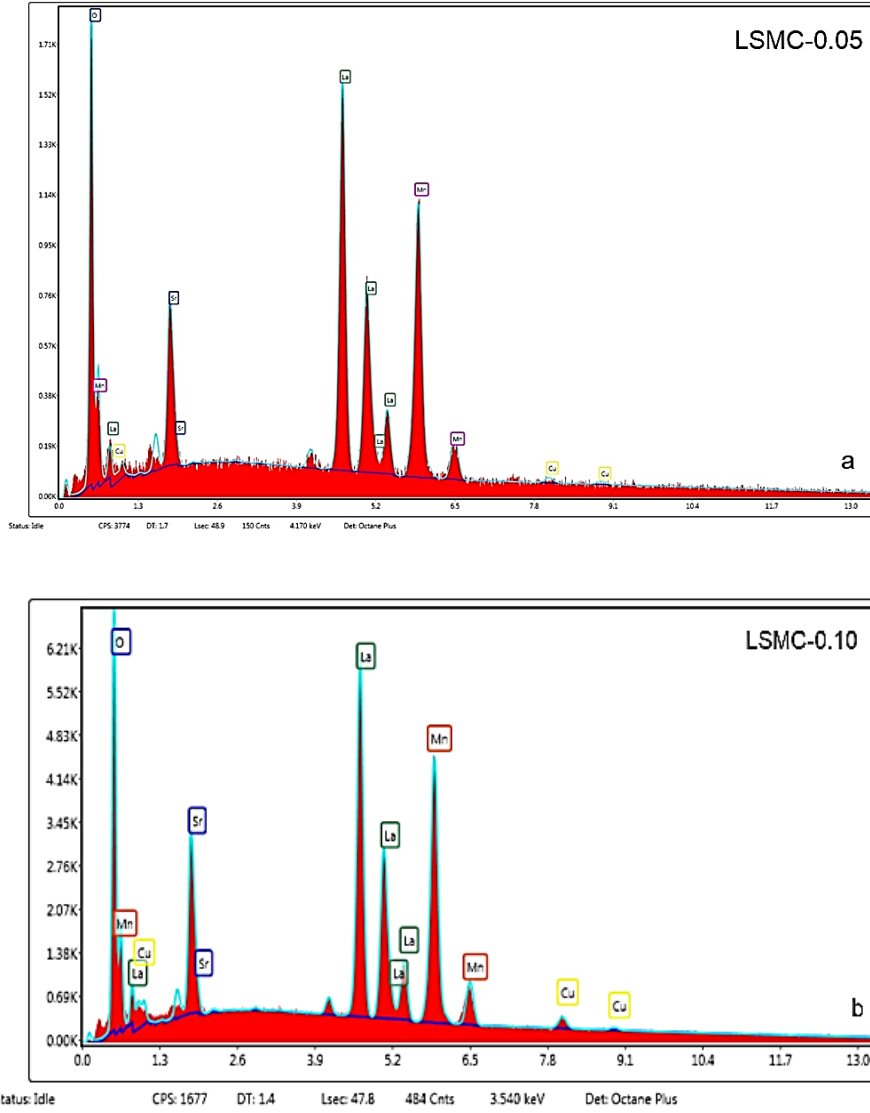
Figure 4: EDS spectra of LSMC-0.05 and LSMC-0.10 samples

Table 2: Atomic percentages of LSMC-0.05 and LSMC-0.10 samples

Sample Code	Atomic percentages %				
	La	Sr	Mn	Cu	O
LSMC-0.05	15.07	4.96	19.61	0.68	59.05
LSMC-0.10	15.29	5.51	19.73	1.47	58.01

To investigate the magnetic behavior dependent on temperature of the samples, magnetization measurements under low magnetic field (10 mT) were carried out in ZFC and FC modes. Thermomagnetic curves of the samples are given in Fig. 5. The $M(T)$ curves of the samples exhibit a transition from the ferromagnetic (FM) to the paramagnetic (PM) phase with the increase in temperature. It is seen that ZFC and FC curves are reversible in the paramagnetic region and
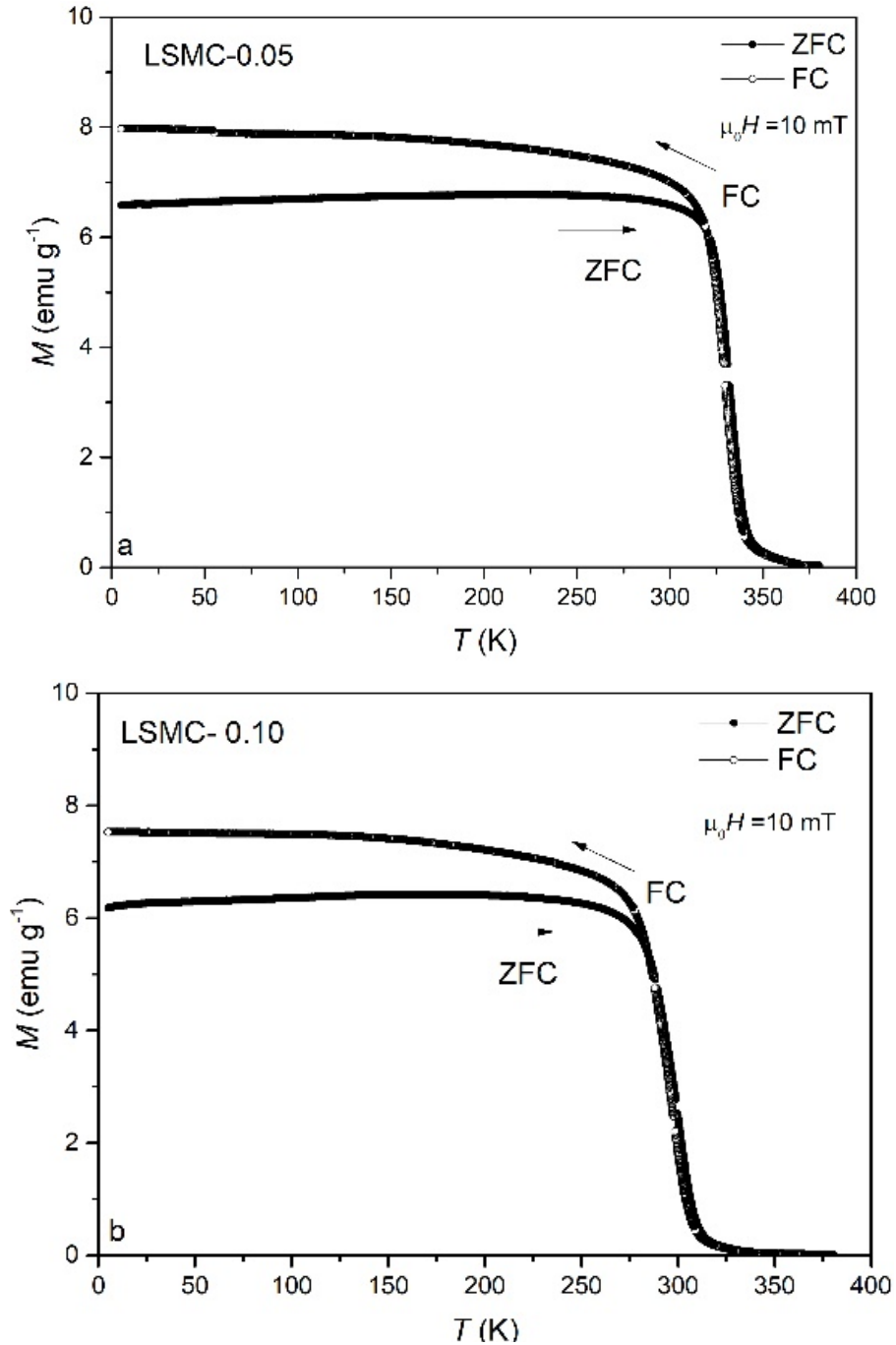
Figure 5: *M (T)* curves of the samples (a) LSMC-0.05 and (b) LSMC-0.10 at ZFC and FC modes

follow an irreversible path by separating from each other in the ferromagnetic region. This separation between the ZFC and FC curves may arise from magnetic anisotropy effect and long-range magnetic interactions [30]. T_C is generally determined from the inflection point of the d$M(T)$/d(T) curve. T_C values of LSMC-0.05 and LSMC-0.10 samples are 330 and 301 K, respectively. In our previous study, the T_C value of the LSM sample synthesized using the same material preparation method was reported as 363 K [26]. It was observed that the transition

temperature decreased when Cu was added to Mn-site. The ratio of Mn^{4+}/ Mn^{3+} ions was calculated as 0.58 and 0.80 for LSMC-0.05 and LSMC-0.10 materials, respectively. According to the results, it was observed that the number of Mn^{4+} increases with the increasing of Cu ratio. This results in decreasing the number of conduction electrons in the structure and T_C decreases. It is known that the change in Mn-O-Mn bond angle and Mn-O bond length causes a change in T_C value [31, 32]. For LSMC-0.05 and LSMC-0.10 samples, Mn-O-Mn bond angle and Mn-O bond length were determined from Rietveld refinement and given in Table 1. The Cu substitution to Mn-site induces a distortion in Mn-octahedra. This distortion limits the mobility of eg electrons [33]. As a result, double exchange interactions weaken and T_C reduces [32, 34]. The magnetic and magnetocaloric properties are also affected by the grain size of the samples as the smaller grain sizes may generate a strain that can disrupt the long-range FM order at the grain boundaries [35]. As mentioned above, the grain size of the samples decreased and the grain boundaries deteriorated with Cu substitution. This result supports the observed decrease in T_C.

In order to examine the magnetization behavior of the samples against the magnetic field, to calculate the magnetic entropy change values and to determine the type of magnetic phase transition, magnetization measurements were carried out depending on the magnetic field. Measurements have been performed below and above T_C of the samples in 4 K increments. The magnetic field has been applied to the samples up to field value of 5 T. The $M(H)$ curves are given in Fig. 6. It is seen that the $M(H)$ curves reach saturation rapidly when a low magnetic field is applied in the low temperature region. The $M(H)$ curves of the samples show a linear variation characteristic of the PM state at temperatures above the T_C.
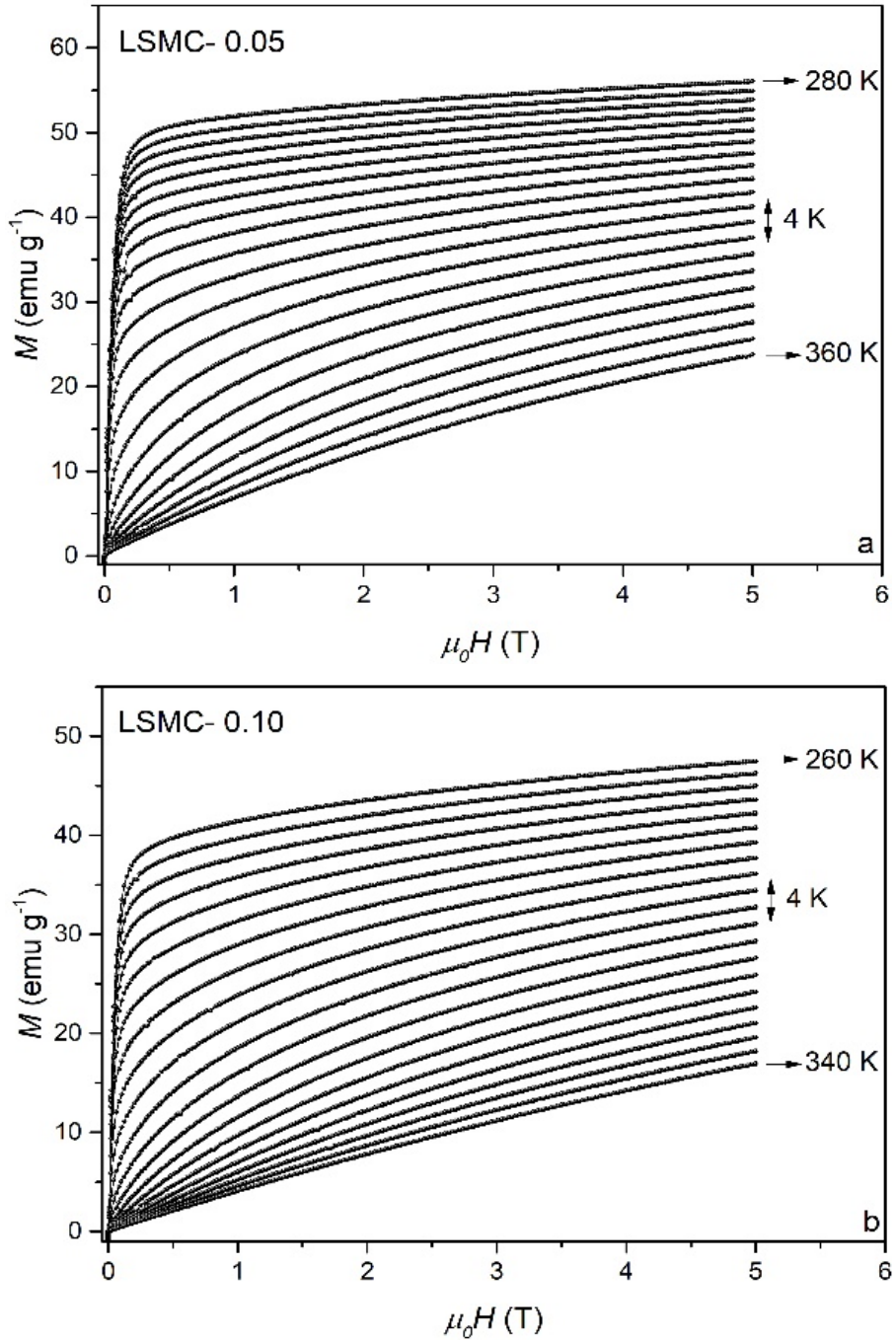
Figure 6: *M*(*H*) curves of the samples (a) LSMC-0.05 and (b) LSMC-0.10

The kind of the magnetic phase transition is quite important for MR applications. The samples exhibiting FOMT show large $-\Delta S_M$ [13]. However, they have large hysteresis (magnetic and thermal), which affects the cooling efficiency and reversibility of a magnetic refrigerant [13]. Therefore, these group materials are not suitable for application. Compared to FOMT, materials showing SOMT have higher potential for use in applications since their thermal and magnetic hysteresis are negligible [16, 17]. The transition takes place over a wider temperature range than

another. For the reasons mentioned above, it is important to specify the type of magnetic phase transition. For identifying the type of magnetic phase transition, Banerjee criterion is generally used and Arrott plots are obtained from $M(H)$ measurements. [36]. Banerjee's criterion says that if the Arrott plots have a positive slope around T_C, the type of the magnetic phase transition is second order. Otherwise, it is first order. We have obtained the Arrott plots as given in Fig. 7. Around T_C, LSMC-0.05 and LSMC-0.10 samples have a positive slope. As a result, one can say that transition is second order.
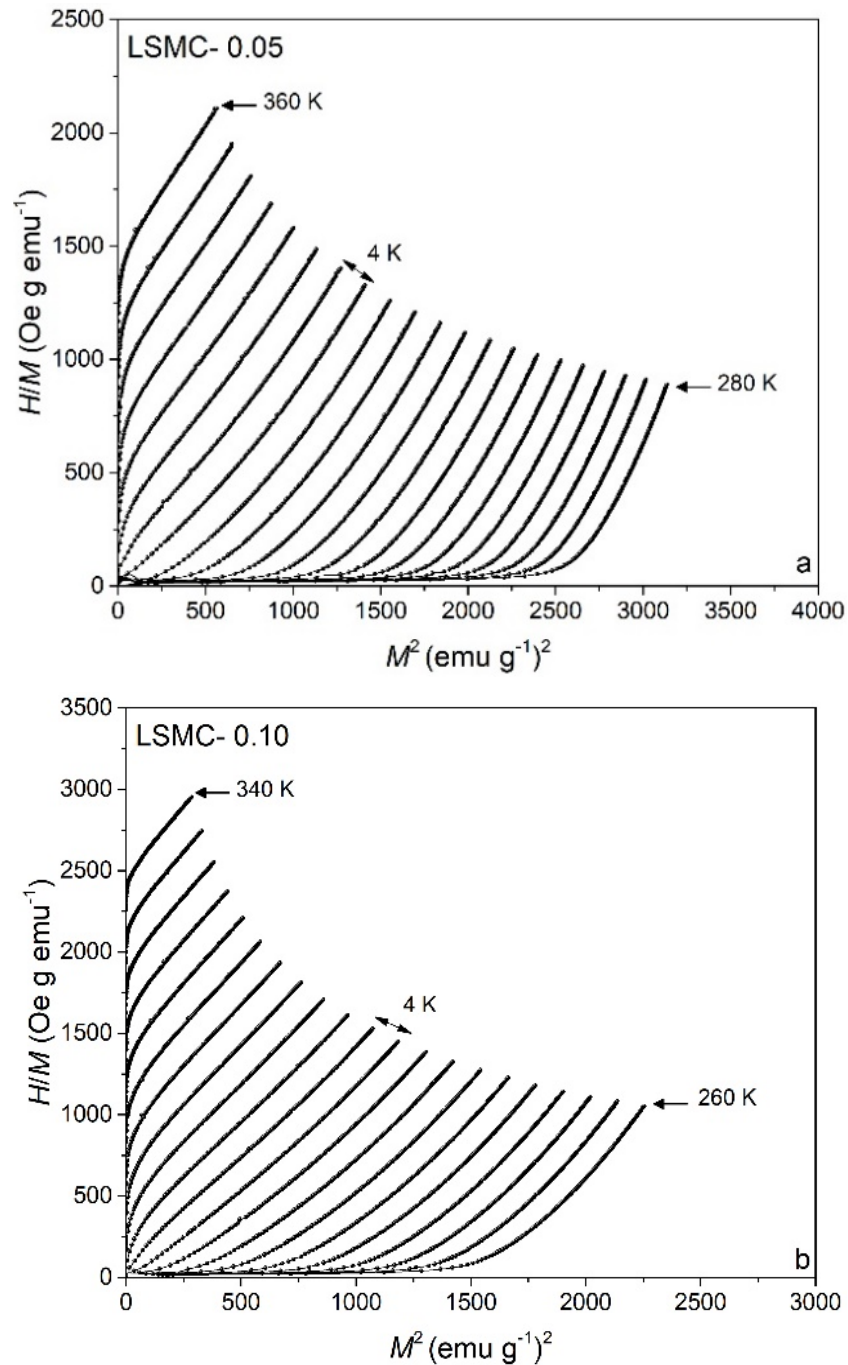
Figure 7: Arrott plot of the samples (a) LSMC-0.05 and (b) LSMC-0.10

$-\Delta S_M$ which is one of the components of MCE is calculated from $M(H)$ curves. Depending on Maxwell's relations and using numerical approximation, it can be practically written as follows [14];

$$-\Delta S_M(H,T) = \sum \frac{M_i - M_{i+1}}{T_{i+1} - T_i} \Delta H_i. \tag{2}$$

M_i and M_{i+1} parameters given in the equation are the magnetization values at T_i and T_{i+1} temperature, respectively. The $-\Delta S_M$ values corresponding to each temperature value of the samples were calculated. Figure 8 shows $-\Delta S_M(T)$ curves describing the temperature dependence of $-\Delta S_M$. The curves show a maximum peak defining maximum magnetic entropy change $(-\Delta S_M^{max})$ near T_C. The value of $-\Delta S_M^{max}$ for the samples has shown an increment with the increasing magnetic field. This is related to the increase in the number of magnetic moments oriented with the applied magnetic field [37]. It can be seen that the location of $-\Delta S_M^{max}$ peak is almost constant and does not show magnetic field dependency. This is observed when the Curie temperature is not dependent on the magnetic field. Otherwise, shifts are observed in the peak position [38]. The $-\Delta S_M^{max}$ values of LSMC-0.05 and LSMC-0.10 samples were calculated as 3.39 and 2.78 Jkg^{-1}K^{-1} under 5 T magnetic fields, respectively. It has been observed that the substitution of Cu to Mn-site causes a decrease in $-\Delta S_M^{max}$ values, as in T_C. It is possible to say that this decrease is related to the decrease of conduction electrons in the structure. Relative cooling power (RCP), called as magnetic cooling efficiency, and is another important parameter for the technological applications of MR systems. Its value can be calculated by the following equation [2];

$$RCP = |-\Delta S_M^{max}| \times \delta T_{FWHM} \tag{3}$$

where δT_{FWHM} is the full width at half maximum of the magnetic entropy curves. For LSMC-0.05 and LSMC-010 samples RCP values were calculated as 249.52 and 111.98 Jkg^{-1}, respectively. RCP value has decreased with increasing of Cu concentration.
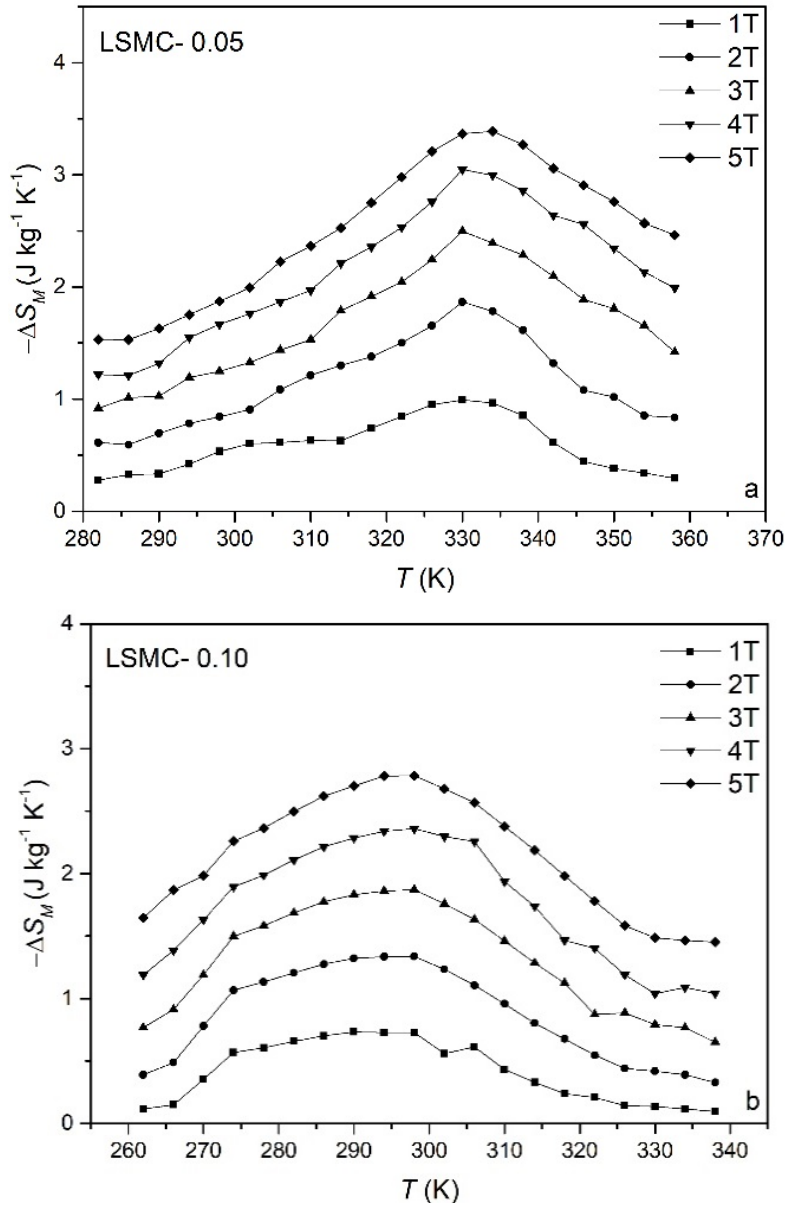
Figure 8: $-\Delta S_M(T)$ of the samples (a) LSMC-0.05 and (b) LSMC-0.10

The state equation of a magnetic system can be written based on the energy minimization as given following [39]:

$$\frac{H}{M} = a(T) + b(T)M^2 + c(T)M^4 \tag{4}$$

In the equation, there is a physical meaning of *a*, *b*, and *c* terms called Landau coefficients which change with temperature. First, the term *a* is related to magnetic susceptibility and is used to determine T_C [32]. The term *b* is related to the order of magnetic phase transition. At T_C, if term *b* has a positive slope, it is second order [40]. The term *c* is a constant. The temperature dependent

variation of *a*, *b* and *c* terms is given in Fig. 9 for LSMC-0.05 and LSMC-0.10 samples. As seen from figures, term *b* has positive value and it confirms that the order of transition is second order.
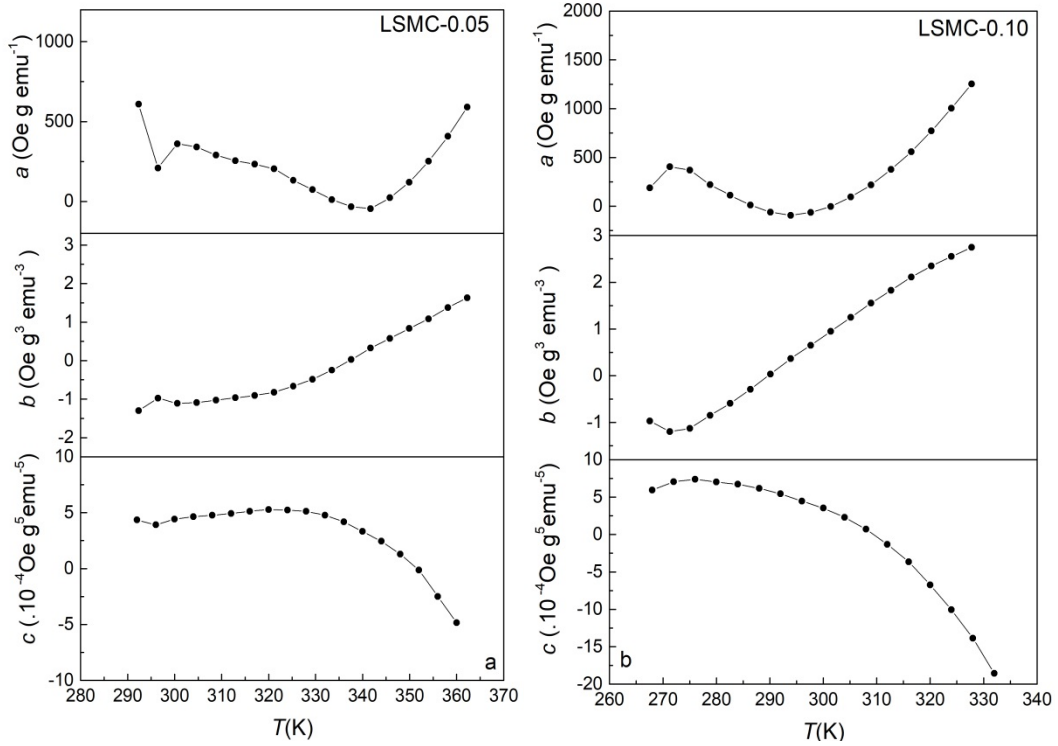
Figure 9: The temperature dependent variation of *a*, *b* and *c* terms for (a) LSMC-0.05 and (b) LSMC-0.10

The $-\Delta S_M$ can be theoretically calculated from following equation [39]

$$-\Delta S_M = \left(\frac{\partial G}{\partial T}\right)_H = \frac{1}{2}a'(T)M^2 + \frac{1}{4}b'(T)M^4 + \frac{1}{6}c'(T)M^6 \tag{5}$$

For both samples, the temperature dependence of the theoretical and experimental $-\Delta S_M$ curves under 5 T is given in Fig. 10. It is seen that there is a small difference between theoretical and experimental values for LSMC-0.05. It is considered that the Jahn–Teller effect, exchange interactions and micromagnetism may induce a difference between theoretical and experimental values of the $-\Delta S_M$ [41]. For LSMC-0.10 sample, the experimental and theoretical values are compatible with each other; this implies that $-\Delta S_M$ values and its temperature dependency are affected by magnetoelastic coupling and electron interactions [42, 43].
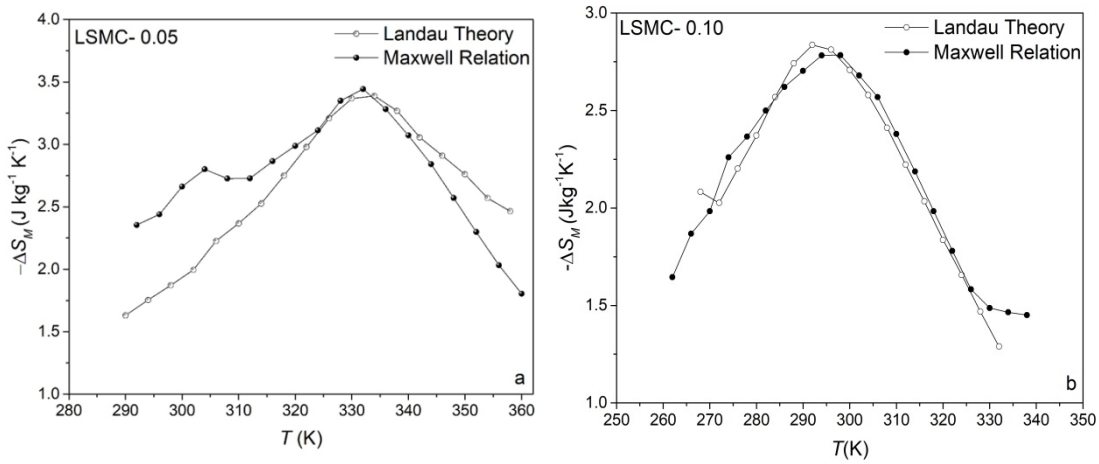
Figure 10: $-\Delta S_M(T)$ of the samples (a) LSMC-0.05 and (b) LSMC-0.10

4. Conclusion

In summary, magnetic and magnetocaloric properties as well as structural properties of LSM0.05 and LSMC-0.10 samples obtained by sol-gel method has been investigated. The structural properties of LSMC-0.05 and LSMC-0.10 samples were determined using XRD. Both samples were crystallized in rhombohedral structure. It is observed that a small change was observed in the lattice parameters and unit cell volume values with the increasing of Cu concentration. A decrement in the grain size and an increment in porosity between grains have been observed with Cu substitution to the Mn-site. The LSMC-0.05 and LSMC-0.10 samples show ferromagnetic- paramagnetic magnetic phase transition at 330 K and 301 K, respectively. It has been confirmed by the Landau and Banerjee criterion that the samples exhibit second-order phase transition. The $-\Delta S_M^{max}$ values of LSMC-0.05 and LSMC-0.10 samples have been calculated as 3.39 and 2.78 Jkg^{-1}K^{-1} under 5 T magnetic fields, respectively. It has been observed that replacing Mn with Cu element in the structure causes a decrease in $-\Delta S_M^{max}$ values as well as in T_C. RCP values were calculated as 249. 52 and 111.98 Jkg^{-1} for LSMC-0.05 and LSMC-010 samples, respectively. According to the results, we can say that the substitution of Cu to the Mn-site negatively affects the magnetic and magnetocaloric properties of the samples.

References

[1] Sari, O., Balli, M., *From conventional to magnetic refrigerator technology*, International Journal of Refrigeration, 37, 8-15, 2014.

[2] Brown, J.S., Domanski, P.A., *Review of alternative cooling technologies, Applied Thermal Engineering*, 64, 252-262, 2014.

[3] Calm, J. M., *Emissions and environmental impacts from air-conditioning and refrigeration systems*, International Journal of Refrigeration, 25, 293-305, 2002.

[4] Omer, A.M., *Energy use and environmental impacts: A general review*, Journal of Renewable and Sustainable Energy, 1, 053101, 2009.

[5] Khosla, R., Miranda, N.D., Trotter, P.A., Mazzone, A., Renaldi, R., McElroy, C., Cohen, F., Jani, A., Perera-Salazar, R., McCulloch, M., *Cooling for sustainable development*, Nature Sustainability, 4, 201-208, 2021.

[6] Crossley, S., Mathur, N., Moya, X., *New developments in caloric materials for cooling applications,* Aip Advances, 5, 067153, 2015.

[7] Akça, G., Kılıç Çetin, S., Ekicibil, A., *Composite $xLa_{0.7}Ca_{0.2}Sr_{0.1}MnO_3/(1-x)$ $La_{0.7}Te_{0.3}MnO_3$ materials: magnetocaloric properties around room temperature*, Journal of Materials Science: Materials in Electronics, 31, 6796–6808, 2020.

[8] Ayaş, A.O., Kılıç Çetin, S., Akyol, M., Akça, G., Ekicibil, A., *Effect of B site partial Ru substitution on structural magnetic and magnetocaloric properties in $La_{0.7}Pb_{0.3}Mn_{1-x}Ru_xO_3$ (x=0.0, 0.1 and 0.2) perovskite system*, Journal of Molecular Structure, 1200, 127120, 2020.

[9] Dhahri, A., Dhahri, J., Dhahri, E., *Effect of potassium doping on physical properties of perovskites $La_{0.8}Cd_{0.2-x}K_xMnO_3$*, Journal of Alloys and Compounds, 489, 9-12, 2010.

[10] Elghoul, A., Krichene, A., Boujelben, W., *Landau theory and critical behavior near the ferromagnetic-paramagnetic transition temperature in $Pr_{0.63}A_{0.07}Sr_{0.3}MnO_3$ (A=Pr, Sm and Bi) manganites*, Journal of Physics and Chemistry of Solids, 108, 52-60, 2017.

[11] Pecharsky, V.K., Gschneidner Jr, K.A., *Magnetocaloric effect and magnetic refrigeration*, Journal of Magnetism and Magnetic Materials, 200, 44-56, 1999.

[12] Biswas, A., Chandra, S., Phan, M.H., Srikanth, H., *Magnetocaloric properties of nanocrystalline $LaMnO_3$: Enhancement of refrigerant capacity and relative cooling power*, Journal of Alloys and Compounds, 545, 157-161, 2012.

[13] Phan, M.H., Yu, S.C., *Review of the magnetocaloric effect in manganite materials*, Journal of Magnetism and Magnetic Materials, 308, 325-340, 2007.

[14] Tishin, A.M., Spichkin, Y.I., *The Magnetocaloric Effect and its Applications*, IOP Publishing LTD, London, 2003.

[15] Franco, V., Conde, A., Kuz'min, M. D., Romero-Enrique, J. M., *The magnetocaloric effect in materials with a second order phase transition: Are T_C and T_{peak} necessarily coincident?*, Journal of Applied Physics 105, 07A917, 2009.

[16] Mleiki, A., Othmani, S., Cheikhrouhou-Koubaa, W., Cheikhrouhou, A., Hlil E. K., *Enhanced relative cooling power in Ga-doped $La_{0.7}(Sr,Ca)_{0.3}MnO_3$ with ferromagnetic-like canted state*, RSC Advances, 6, 54299–54309, 2016.

[17] Lyubin, J., *Magnetocaloric materials for energy efficient cooling*, Journal of Physics D: Applied Physics, 50, 053002, 2017.

[18] Paticopoulos, S.C., Caballero-Flores, R., Franco, V., Bla´zquez, J.S., Cond, A., Knipling, K.E., Willard, M.A., *Enhancement of the magnetocaloric effect in composites: Experimental validation*, Solid State Communications, 152 , 1590–1594, 2012.

[19] Monfared, B. Palm, B., *Material requirements for magnetic refrigeration applications*, International Journal of Refrigeration, 96, 25–37,2018.

[20] Coey, J. M. D., Viret, M., Von Molnár, S., *Mixed-valence manganites*, Advances in Physics, 48:2, Taylor & Francis, 167-293, 1999.

[21] Rostamnejadi A., Salamati, H., Kameli, P., Ahmadvand, H., *Superparamagnetic behavior of $La_{0.67}Sr_{0.33}MnO_3$ nanoparticles prepared via sol–gel method*, Journal of Magnetism and Magnetic Materials, 321, 3126–3131, 2009.

[22] Zverev, V.I., Pyatakov, A.P., Shtil, A.A., Tishin, A.M., *Novel applications of magnetic materials and technologies for medicine*, Journal of Magnetism and Magnetic Materials, 459, 182–186, 2018.

[23] Thaljaou, R., Boujelben, W., Pekała, M., Pekała, K., Mucha, J., Cheikhrouhou, A., *Structural, magnetic and transport study of monovalent Na-doped manganite $Pr_{0.55}Na_{0.05}Sr_{0.4}MnO_3$*, Journal of Alloys and Compounds, 558, 236–243, 2013.

[24] Levy, P., Parisi, F., Polla, G., Vega, D., Leyva, G., Lanza, H., *Controlled phase separation in $La_{0.5}Ca_{0.5}MnO_3$*, Physical Review B, 62, 6437-6441, 2000.

[25] Walha, I., Smari, M., M'nasri, T., Dhahri, E., *Structural, magnetic, and magnetocaloric properties of Ag-doped in the $La_{0.6}Ca_{0.4}MnO_3$ compound*, Journal of Magnetism and Magnetic Materials, 454, 190–195, 2018.

[26] Kılıç Çetin, S., Akça, G., Aslan, M. S., Ekicibil, A., *Role of nickel doping on magnetocaloric properties of $La_{0.7}Sr_{0.3}Mn_{1-x}Ni_xO_3$ manganites*, Journal of Material Science: Materials in Electronics, 32,10458–10472, 2021.

[27] Goldschmit, V.M*., Geochemische Verteilungsgesetz der Element 7*, Kristiania, Oslo, 1923-1938.

[28] Bhalla, A. S., Guo, R., Roy, R., T*he Perovskite Structure - a Review of its Role in Ceramic Science and Technology*," Material Research Innovations 4, 3–26, 2000.

[29] Shannon, R.D. , *Revised effective ionic radii and systematic studies of interatomic distances in halides and chalcogenides,* Acta Crystallographica A 32:5, 751–767, 1976.

[30] Kılıç Çetin, S., Acet, M., Ekicibil, A., *Effect of Pr-substitution on the structural, magnetic and magnetocaloric properties of $(La_{1-x}Pr_x)_{0.67}Pb_{0.33}MnO_3$ $(0.0 \leq x \leq 0.3)$ manganites*, Journal of Alloys and Compounds, 727, 1253-1262, 2017.

[31] Sfifir, I., Ezaami, A., Cheikhrouhou-Koubaa, W., Cheikhrouhou, A., *Structural, magnetic and magnetocaloric properties in $La_{0.7-x}Dy_xSr_{0.3}MnO_3$ manganites (x = 0.00, 0.01 and 0.03)*, Journal of Alloys and Compounds (696), 760–767, 2017.

[32] Akça, G., Kılıç Çetin, S., Ekicibil, A., *Structural, magnetic and magnetocaloric properties of $(La_{1-x}Sm_x)_{0.85}K_{0.15}MnO_3$ (x = 0.0, 0.1, 0.2 and 0.3) perovskite manganites*, Ceramics International, 43, 15811–15820, 2017.

[33] Bouzaiene, E., Dhahri, J., Hlil, E. K., Belmabrouk, H., Alrobei, H., *Three-dimensional Heisenberg critical phenomena in $La_{0.6}Bi_{0.1}Sr_{0.3-x}Ca_xMn_{0.9}Cu_{0.1}O_3$ manganites (x = 0 and 0.05)*, Journal of Material Science: Materials in Electronics ,31, 18186–18197, 2020.

[34] Zhang, T., Wang, X. P., Fang, Q. F., Li, X. G., *Magnetic and charge ordering in nanosized manganites*, Applied Physics Reviews, 1, 031302, 2014

[35] M'nassri, R., Boudjada, N. C., Cheikhrouhou, A., *Impact of sintering temperature on the magnetic and magnetocaloric properties in $Pr_{0.5}Eu_{0.1}Sr_{0.4}MnO_3$ manganites*, Journal of Alloys and Compounds, 626, 20–28, 2015.

[36] Banerjee, B.K., *On a generalised approach to first and second order magnetic transitions*, Physics Letters, 12, 16–17, 1964.

[37] Mansouri, M., Omrani, H., Cheikhrouhou-Koubaa, W., Koubaa, M., Madouri, A., Cheikhrouhou, A., *Effect of vanadium doping on structural, magnetic and magnetocaloric properties of $La_{0.5}Ca_{0.5}MnO_3$*, Journal of Magnetism and Magnetic Materials, 401, 593–599, 2016.

[38] Zhang, L., Li, L., Li, R., Fan, J., Ling, L., Tong, W., Qu, Z., Tan, S., Zhang, Y., *Spin–lattice coupling studied by magnetic entropy and EPR in the $CdCr_2S_4$ system*,Solid State Communications, 150, 2109–2113, 2010.

[39] Amaral, V.S., Amaral, J.S., *Magnetoelastic coupling influence on the magnetocaloric effect in ferromagnetic materials*, Journal of Magnetism and Magnetic Materials, 272–276, 2104–2105, 2004.

[40] Amaral, V.S., Araújo, J.P., Pogorelov, Y. G., Tavares, P.B., Sousa, J.B, Vieira, J.M., *Discontinuous transition effects in manganites: magnetization study in the paramagnetic phase*, Journal of Magnetism and Magnetic Materials, 242–245, 655–658, 2002.

[41] Yang, H., Zhang, P., Wu, Q., Ge, H., Pan, M., Effect of monovalent metal substitution on the magnetocaloric effect of perovskite manganites $Pr_{0.5}Sr_{0.3}M_{0.2}MnO_3$ (M=Na, Li, K and Ag), Journal of Magnetism and Magnetic Materials, 324, 3727–3730, 2012.

[42] Koubaa, M., Regaieg, Y., Koubaa, W.C., Cheikhrouhou, A., Ammar-Merah, S., Herbst, F., Magnetic and magnetocaloric properties of lanthanum manganites with monovalent elements doping at A-site, Journal of Magnetism and Magnetic Material, 323, 252–257, 2011.

[43] Cherif, R., Hlil, E.K., Ellouze, M., Elhalouani, F., Obbade, S., Study of magnetic and magnetocaloric properties of $La_{0.6}Pr_{0.1}Ba_{0.3}MnO_3$ and $La_{0.6}Pr_{0.1}Ba_{0.3}Mn_{0.9}Fe_{0.1}O_3$ *perovskite-type manganese oxides*, Journal of Material Science, 49, 8244–8251, 2014.